

Hot spots and burning times: A spatiotemporal analysis of calls for service to establish police demand

Maite Dewinter^{1,*}, Christophe Vandeviver^{2,3}, Philipp M. Dau², Tom Vander Beken², and Frank Witlox^{1,4,5}

Maite Dewinter: maite.dewinter@ugent.be, +32 9 264 46 29, ORCID: 0000-0001-7430-462X,
*Corresponding author

Christophe Vandeviver: christophe.vandeviver@ugent.be, +32 9 264 97 03, ORCID: 0000-0001-9714-7006, [linkedin.com/in/christophevandeviver](https://www.linkedin.com/in/christophevandeviver)

Philipp M. Dau: philippmartin.dau@ugent.be, + 32 9 264 69 46, ORCID: 0000-0001-6739-9878, [linkedin.com/in/philipp-dau-69578b150](https://www.linkedin.com/in/philipp-dau-69578b150)

Tom Vander Beken: tom.vanderbeken@ugent.be, +32 9 264 69 39, ORCID: 0000-0002-1596-5070, [linkedin.com/in/tom-vander-beken-29814821](https://www.linkedin.com/in/tom-vander-beken-29814821)

Frank Witlox: frank.witlox@ugent.be, +32 9 264 45 53, ORCID: 0000-0002-8966-6823, [linkedin.com/in/frank-witlox-05b634](https://www.linkedin.com/in/frank-witlox-05b634)

Abstract

Establishing police demand is important to optimally allocate scarce police resources in space and time. To contribute to the existing knowledge on the optimization of policing and crime prevention strategies worldwide, we examine the spatiotemporal pattern of calls for service (CFS), with a focus on the urgency of the calls (as measured by the police priority codes), in Antwerp (2017-2020), Belgium. To disentangle the space-time pattern of the priority codes, we apply the average nearest neighbour statistic, global and local Moran's I, Getis-Ord G_i^ , and emerging hot spot analysis. Our results demonstrate that the spatial, temporal, and space-time patterns of the priority codes differ and that more urgent CFS are more demanding in terms of allocated police vehicles than less urgent CFS. Based on the findings of this paper, we recommend to include priority codes in future police patrol routing solutions to make patrol strategies more realistic. An important aspect will be to increase/decrease the number of available units depending on the spatiotemporal pattern of the CFS per priority code. Instead of only working with fixed shifts, there is a need to deploy peak shifts during times of peak demand.*

Keywords: Priority; Exploratory (spatial) data analysis; micro level; space-time pattern; LISA; Antwerp (Belgium)

1. Introduction

¹ Department of Geography, Ghent University

² Department of Criminology, Criminal Law and Social Law, Ghent University

³ Research Foundation-Flanders (FWO)

⁴ Department of Geography, University of Tartu

⁵ College of Civil Aviation, Nanjing University of Aeronautics and Astronautics

36

37 Over the last two decades, both geographers and criminologists gained more interest in the geography
38 of crime and crime prevention, instead of just focusing on characteristics of the offender (Helbich &
39 Leitner, 2017; Newton & Felson, 2015; Vandeviver & Bernasco, 2017). In 1989, Sherman et al.
40 observed that 50.4% of all calls for service (CFS) in Minneapolis (United States) for which a police car
41 was dispatched were concentrated in 3.3% of all addresses and intersections. Their research was
42 influential, since it marked the first analysis of CFS on a micro scale, which was, among other things,
43 facilitated by the increasing number of police stations equipped with computer aided dispatch systems
44 (Lee et al., 2017; Sherman et al., 1989; Sherman, 1995). The introduction of national emergency
45 numbers along with developments in data recording, storage, and analysis suddenly provided the police
46 with reliable information on the time and place of an incident, and captured many events which were
47 not shown in, e.g., crime reports (Luan et al., 2016; Mastrofski, 1990; Sherman et al., 1989; Wain &
48 Ariel, 2014). Sherman et al. (1989) state that: “Calls to the police provide the most extensive and faithful
49 account of what the public tells the police about crime, with the specific errors and biases that that
50 entails” (Sherman et al., 1989, p. 36). Consequently, CFS act in this paper as the demand for police
51 service from the public, in time and space, to which the supply of police resource should be matched
52 (Bowers, 1999). Over or under supply of police presence can be inefficient and potentially harmful
53 because incident response times may become too long or the intensity of certain hot spots can become
54 excessive in the absence of police surveillance (Davies & Bowers, 2019; Mukhopadhyay et al., 2016).
55 It can also affect people’s fear of crime and feeling of safety (Dau et al., 2021b).

56

57 Laufs et al. (2020) discuss five drivers of police demand: (1) *the baseline*, the minimum level of police
58 resource to remain operational (context dependent), (2) *cyclical factors*, drivers with discrete dates, such
59 as large-scale cultural events, (3) *the seasons* of the year, (4) *one off incidents*, for example, natural
60 disasters, a large sporting event, or the marginalisation of certain groups after a specific incident (e.g.,
61 terrorist attack), and (5) *(localised) emerging trends*, ‘new types or forms of crime, or non-crime
62 problem, that were previously unseen (at least in the local context) but that suddenly take up
63 disproportionate amounts of resources [...]’ (Laufs et al., 2020, p. 10). As stated by Laufs et al. (2020)
64 based on these five drivers, police demand is surely not a static measure.

65

66 To optimally deploy police officers in the field, in other words, to match demand and supply, officers
67 and police chiefs not only have to know where a CFS will occur, but also when it will occur (Townsend,
68 2008). Initially, the geography of crime was dominated by a focus on the spatial characteristics of crime,
69 but over the past years its temporal component is addressed as well and the lessons that can be learned
70 from these analyses to improve crime control activities (Hu et al., 2018; Luan et al., 2016; Shiode et al.,
71 2015; Spicer et al., 2016; Weisburd et al., 2006; Ye et al., 2015). Therefore, geographical analysis and
72 crime mapping are important aspects of police work in its evidence-based and data driven transition

73 during the last two decades (Dau et al., 2021a) and have the ability to optimize the targeted management
74 of police officers in time and space (Chen et al., 2017; Dewinter et al., 2020; Watanabe & Takamiya,
75 2014).

76

77 With space-time studies in North America, Brazil, and other countries around the world the
78 generalizability of the law of crime concentration or the routine activity theory increases (de Melo et al.,
79 2015) and ‘have led to the accumulation of new findings on the space-time signature of different types
80 of crime’ (Shiode et al., 2015, p. 697). We want to contribute to this by analysing the space, time, and
81 space-time pattern of police demand in Antwerp (Belgium), more specifically, with a focus on
82 prioritization of CFS. In the case of the Antwerp police, the CFS are dispatched to the officers
83 accompanied by a code indicating the urgency of the incident. This code, the priority code, is assigned
84 by the dispatch centre and gives an indication of the severity of an incident. Depending on the priority
85 code, response times should be minimized. The most critical incidents, e.g., life-threatening incidents,
86 are given priority over less serious ones and officers are allowed to use their siren and flashing lights to
87 clear the right of way and thus reduce response times. Police officers act firstly based on the priority and
88 only secondly on the type of incident and “[...] *in the process of identifying geographical areas that are*
89 *to be prioritized for patrolling, it is irrational to value serious assault and verbal harassment equally*”
90 (Kärholm et al., 2020, p. 16). Nevertheless, this aspect of police patrol is underexposed in
91 spatiotemporal analysis of crime or CFS data.

92

93 Most papers focus on specific types of recorded crime or CFS, hence, they can only make a statement
94 about these crimes/incidents (Boivin, 2018; Chun, 2014; Chung & Kim, 2019; Curtis-Ham & Walton,
95 2017; Hu et al., 2018; Nelson et al., 2001; Shiode et al., 2015). Moreover, among others in our study
96 area there is a difference between the two data sets. *CFS* contain offences or incidents reported to the
97 police by the public to which police officers were dispatched. *Recorded crime* consists of reports
98 generated by officer-initiated activity and CFS that have resulted in an official police report. For
99 example, De Melo et al. (2015) applied the spatial point pattern test to a crime data set with sixteen
100 different classifications (categorised as robbery, theft and rape). On the street segment level, the spatial
101 patterns of these crime types exhibited spatial similarity. Other examples are the analysis of crime and
102 crash data in order to define optimal patrol routes to reduce the total dispatch time (Kuo et al., 2013) or
103 the application of spatial analysis techniques to analyse the crime deterrent effect of police stations
104 (Fondevila et al., 2021). The space-time analysis techniques used in these studies are valuable, but the
105 approach differs from what we want to achieve in this paper by focusing on CFS and priority codes.
106 Shiode et al. (2015) examine by means of a network-based space-time search window technique the
107 space-time characteristics of robbery, burglary, drug-related crime, and vehicle theft, and managed to
108 identify different types of hotspots (i.e., persistent warm spots and a short-term outburst). The same
109 crime types, with the addition of (sexual) assault, are analysed in Boivin (2018) to test routine activity

110 theory. Geographical weight regression modelling demonstrated that, for these crime types, a large
111 population can be associated with increased as well with decreased levels of crime. In general, burglary,
112 robbery, theft, and violent crime turn out to be popular crimes to investigate in time and space literature
113 (Chun, 2014; Chung & Kim, 2019; Curtis-Ham & Walton, 2017; Hu et al., 2018). Moreover, the scale
114 of research has improved tremendously during the last 30 years (Nelson et al., 2001; Valente, 2019), but
115 some analysis techniques (Chun, 2014; Chung & Kim, 2019) or data availability (Boivin, 2018; Megler
116 et al., 2014) prevent analysis on individual address or street segment level. Thus, many studies perform
117 analysis on aggregated data, e.g., census tract level or on a higher temporal scale, e.g., months or seasons
118 (Andresen & Malleon, 2013). We do not want to detract from the contribution that these studies make
119 to the literature, but we would like to highlight a gap in the literature that we will address in this paper:
120 the space-time analysis of CFS data with a focus on the priority codes. The research question of interest
121 in this paper is whether there is a difference in the space-time patterns of incidents with a different
122 priority code? This information can then be used for the daily operation of police patrol.

123

124 This paper is organised as follows. First, an overview is given of the data set and the methods used to
125 analyse the space-time patterns of the CFS. Second, the Results Section consists of three parts,
126 discussing the main (1) space, (2) time, and (3) space-time patterns, followed by the Discussion and
127 Conclusion Sections.

128

129 **2. Data and Methods**

130

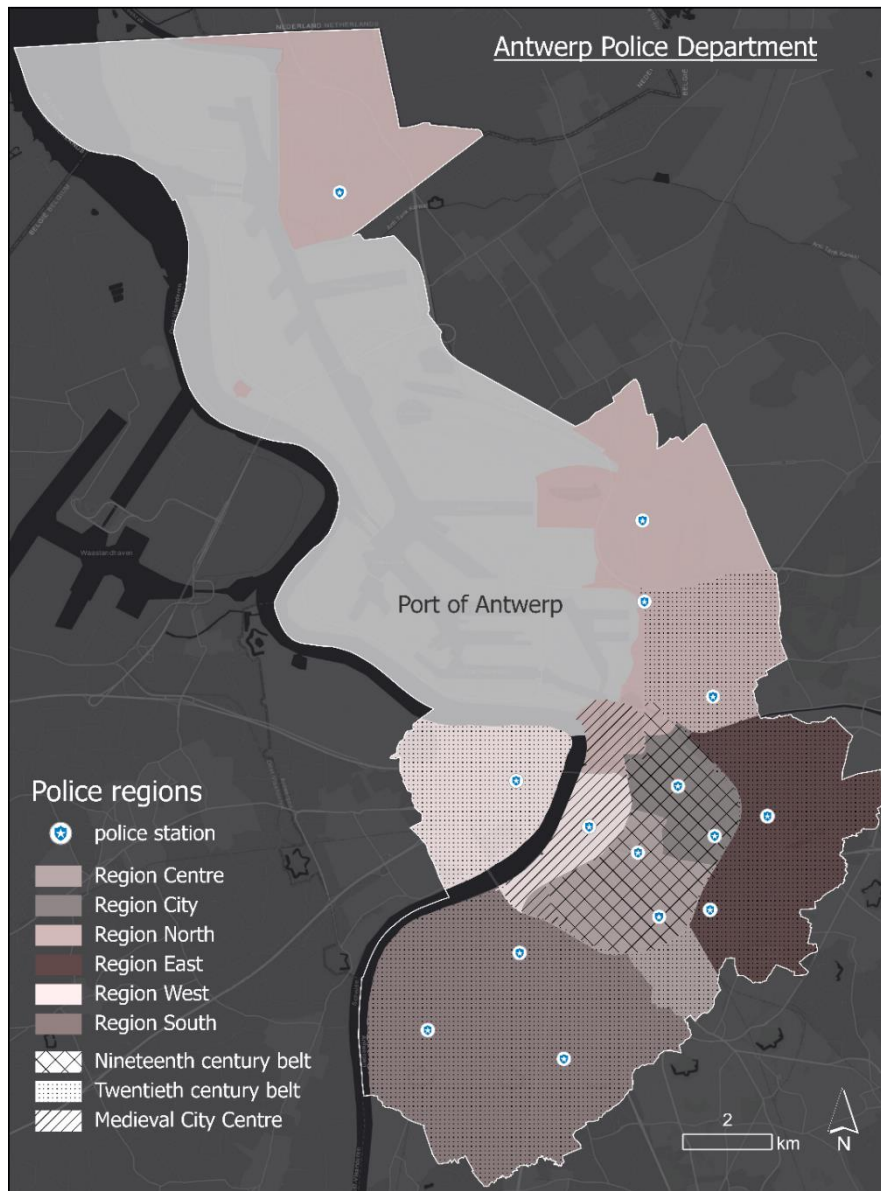
131 *2.1. Antwerp: CFS data and the road network*

132

133 Antwerp's police force is responsible for the safety of 530,104 inhabitants (2020), spread over an area⁶
134 of ca. 204 km². We focus on CFS obtained from the emergency response unit. These officers are
135 dedicated to emergency call response and engage in proactive police patrol: visible or marked patrol in
136 order to prevent crime and maintain social order (Wain & Ariel, 2014). The Antwerp Police Department
137 (APD) is the largest local police force in Belgium in terms of personnel and is divided in six zones. The
138 West region is spread over the right and left bank of the river Scheldt, also stretching over the old
139 medieval city centre (see Fig. 1). City and Centre are both located in the nineteenth century belt of
140 Antwerp and are characterized by densely built neighbourhoods, and zones North, East, and South are
141 situated in the twentieth century belt. Unfortunately, we have no insight into all incidents that take place
142 in the port area because the port falls under the jurisdiction of the Belgian *Federal Police*. Thus only the
143 CFS in which an officer from the APD was involved, are included for analysis.

144

⁶ 72 km² is occupied by the seaport.



145

146

Fig. 1. Antwerp Police Department

147

148 Within a four-year period (2017-2020), 560,580 CFS occurred. The CFS data set contains detailed
 149 information about the time, place, and priority code of each incident. Each CFS receives a priority code
 150 (prio) that is inversely proportional to the urgency and ranges from zero to four. Highly urgent, life-
 151 threatening incidents, requiring immediate intervention receive code zero, and officers are allowed to
 152 use the vehicle's siren and/or flashing lights in order to minimize response time. This is the period
 153 between when a CFS is recorded and the time the first police vehicle arrives on site (Dewinter et al.,
 154 2020). Very low urgency incidents, such as parking violations, receive code four. In total, our data
 155 consists of 2,160 highly urgent, life-threatening incidents that require immediate intervention (0.39%;
 156 prio 0) and 7,953 prio 1 incidents (1.42%; absolute priority without direct risk to someone's life), in
 157 comparison to 156,628 prio 2 (27.94%; urgent and risk of escalation), 292,683 prio 3 (52.21%; routine
 158 (traffic) intervention), and 101,118 prio 4 incidents (18.04%).

159

160 All CFS were geocoded and matched to one of the 31,147 street segments in Antwerp. A street segment
161 is defined as the section of a street between two intersections, and can be, e.g., a part of the highway or
162 an unpaved road in a park as well. We have deliberately chosen to include all the different types of
163 segments in the data set, because they are all part of the public domain; the working area of the police.
164 By focusing on such a small unit of analysis, we are able to minimize aggregation bias (Vandeviver &
165 Steenbeek, 2019).

166

167 2.2. *Methods*

168

169 Exploratory (spatial) data analysis (EDA) is applied to detect space-time patterns and possible
170 anomalies. Therefore, a range of descriptive and spatial statistics, and space-time pattern mining tools
171 are performed on the data set by using R (version 4.0.1) and ArcGIS Pro⁷ (version 2.7.1)
172 interchangeably. A straightforward method to conduct EDA does not exist, but based on existing
173 research on space-time patterns of CFS data or crime data, we perform several techniques (Andresen,
174 2017; Anselin et al., 2000; Felson & Poulsen, 2003; Herrmann, 2013, 2015). The analyses are divided
175 in three parts, first we focus on the spatial characteristics of the data set, second on the time aspects, and
176 third, the findings on space and time are integrated in emerging hot spot analysis.

177

178 2.2.1 Spatial statistics

179 The data set consists of point features, where each point represents an event (an incident). On this micro
180 level of analysis, the focus is on the presence or absence of an incident rather than on some measured
181 attribute. To know which spatial pattern the incidents exhibit, the average nearest neighbour (ANN)
182 statistic is used. This statistic calculates the observed mean distance (\bar{D}_O), this is the average of the
183 distances from each point to its nearest neighbour (d_i), and compares this to the average expected
184 distance (\bar{D}_E) in the case of a random distribution of the points. The nearest neighbour index is equal to
185 the ratio of the observed to the expected mean distance. The pattern exhibits clustering if the index is
186 less than 1, and dispersion if greater than 1. In (1), n corresponds to the total number of CFS, and A is
187 the area of Antwerp (Antrop et al., 2013).

188

$$189 \quad ANN = \frac{\bar{D}_O}{\bar{D}_E} = \frac{\frac{\sum_{i=1}^n d_i}{n}}{\frac{0.5}{\sqrt{n/A}}} \quad (1)$$

190

191 Because police patrol street segments and some spatial tools require aggregated data instead of point
192 data, each incident is matched to its corresponding street segment and the frequency of CFS at each

⁷ ESRI, ArcGIS desktop: Release, 2.7.1. Redlands, CA: Environmental Systems Research Institute, 2021

193 street segment is counted. We use the Global Moran's I statistic to test for spatial autocorrelation. Global
 194 Moran's I ranges from -1, indicating negative spatial autocorrelation or a dispersed pattern, to +1,
 195 meaning positive spatial autocorrelation or a tendency towards a clustered spatial pattern, if the z-score
 196 and p-value are statistically significant. A value equal to zero represents a random pattern (Goodchild,
 197 1986). To determine the threshold distance which reflects maximum spatial autocorrelation, we first run
 198 the incremental spatial autocorrelation tool in ArcGIS Pro. The outcome of this analysis is displayed in
 199 a line graph, where a peak in z-score indicates the threshold distance in which the spatial autocorrelation
 200 is most pronounced.

201

202 Since the Moran's I statistic is a global statistic, which only tells whether the spatial pattern is clustered,
 203 dispersed or random, and not where potential clusters of, in our case, street segments with high or low
 204 values are located, we also apply the Local Moran's I statistic. This statistic shows where statistically
 205 significant clusters of high (high-high cluster) and low (low-low cluster) values, as well as, where
 206 outliers are located. A value is considered to be a statistically significant spatial outlier if the street
 207 segment has a high frequency of CFS and the surrounding segments all have low frequencies (HL), or
 208 the other way around, if a segment with a low frequency is surrounded by segments with high
 209 frequencies (LH). Another local indicator of spatial association statistic (LISA) is Getis-Ord G_i^* (G_i^*)
 210 or (optimized) hot spot analysis. This statistic calculates, given a set of weighted features, statistically
 211 significant hot and cold spots of incidents (Andresen, 2017; Anselin, 1995; Anselin et al., 2000). Getis-
 212 Ord G_i^* only identifies clusters of high-high (high z-score and small p-value) and low-low (low negative
 213 z-score and small p-value) local incidents (Getis & Ord, 1992; Ord & Getis, 1995). We compare G_i^* to
 214 the outcome of Local Moran's I. Both can be shown on a map (Andresen, 2017; Anselin, 1995). All
 215 these spatial statistics are calculated in ArcGIS Pro, using the Spatial Statistics Toolbox.

216

$$217 \quad \text{Global } I = \frac{n \sum_{i=1}^n \sum_{j=1}^n w_{i,j} z_i z_j}{S_0 \sum_{i=1}^n z_i^2} \quad (2)$$

218

$$219 \quad \text{Local } I = \frac{x_i - \bar{X}}{S_i^2} \sum_{j=1, j \neq i}^n w_{i,j} (x_j - \bar{X}) \quad (3)$$

220

$$221 \quad G_i^* = \frac{\sum_{j=1}^n w_{i,j} x_j - \bar{X} \sum_{j=1}^n w_{i,j}}{S \sqrt{\frac{[n \sum_{j=1}^n w_{i,j}^2 - (\sum_{j=1}^n w_{i,j})^2]}{n-1}}} \quad (4)$$

222

223 2.2.2 Time pattern analysis

224 Not a single hot spot is hot 24/7, 52 weeks a year. To know at what time of the day hot streets or areas
 225 are 'hot', we examine the time pattern of the CFS by creating a time heat map (Herrmann, 2013, 2015).
 226 This specific type of heat map is a graphic, which displays the number (full data set) or proportion
 227 (priority codes) of CFS for each day of the week (y-axis) and for each hour of the day (x-axis).

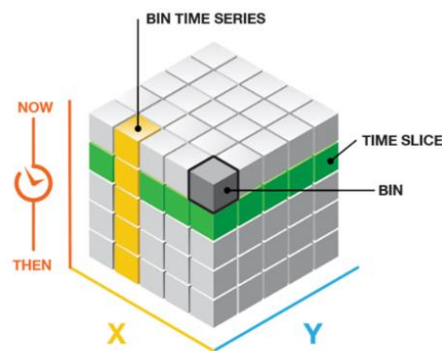
228 Consequently, potential time patterns in the data set become visible. Moreover, we also establish the
229 median minute of crime, crime quartiles, crime's daily timespan, and the, e.g., 5-to-5 share of offenses
230 (Felson & Poulsen, 2003). The median minute of incidents is 'that minute of the day by which exactly
231 half of the incidents have occurred' (Felson & Poulsen, 2003, p. 597). The incident quartiles are those
232 minutes of the day by which a quarter and 75% of the CFS took place. The number of minutes between
233 these two periods is the daily timespan or the inter-quartile range. A higher timespan is generated when
234 CFS are more dispersed over the day. Last, the 5-to-5 share of offenses analyses the proportion of CFS
235 occurring between 5:00 AM and 4:59 PM. This is used to determine the time pattern throughout the day;
236 a lower proportion of CFS indicates a later incident pattern (Ashby & Bowers, 2013; Felson & Poulsen,
237 2003). To analyse potential variability in the time patterns of the days of the week, we extend Felson
238 and Poulsen's (2003) approach by calculating the parameters for each day separately.

239

240 2.2.3 Space-time Pattern Mining: Emerging Hot Spot Analysis

241 To visualize the space-time pattern of the CFS the space-time pattern mining tool 'Emerging Hot Spot
242 analysis' is applied. Before it is possible to run this tool on the data set, a space-time cube, as shown in
243 Fig. 1, is created by aggregating the incident points. To create these space-time cubes, the CFS are
244 aggregated⁸ in hexagons with a diameter of 300 m. This diameter ensures that each hexagon contains
245 sufficient CFS while minimizing the effect of aggregation bias (Fotheringham & Wong, 1991). By
246 creating a space-time cube (netCDF data structure) data can be visualized in three dimensions: the x and
247 y dimensions represent space and a third axis represents time (Esri ArcGIS Pro, n.d.).

248



249

250 **Fig. 2.** Example of a space-time cube (Source: Esri ArcGIS Pro (n.d.)).

251

252 The cube is made up of small 'bins', which can have the same location ID or the same time-step ID.
253 Bins with the same location ID are associated with the same area in space and will represent a time
254 series. A time slice contains bins with the same time-step ID, i.e., these bins are associated with the same
255 time-step interval. Subsequently, this space-time cube is used by the emerging hot spot analysis tool to

⁸ This is automatically done in ArcGIS Pro.

256 identify hot spots in space and time. The statistic that will be calculated for each bin is a space-time
 257 implementation of Getis-Ord G_i^* (Esri ArcGIS Pro, n.d.). The bins that will be included in each analysis
 258 neighbourhood of the Getis-Ord G_i^* statistic are determined by the conceptualization of the spatial
 259 relationships and the neighbourhood time-step value (default settings are used). The eventual hot and
 260 cold spot trends are evaluated by the Mann-Kendall trend test, a rank correlation analysis. Eventually,
 261 each time series will be identified as a new, consecutive, intensifying, persistent, diminishing, sporadic,
 262 oscillating, or historical hot or cold spot. The output of this tool can be visualized in 2D and in 3D (Esri
 263 ArcGIS Pro, n.d.).

264

265 3. Results

266

267 3.1 The spatial pattern of police demand on point and street segment level

268

269 The observed mean distance of the ANN statistic for the full data set (all incidents 2017-2020) is 0.59
 270 meters and the expected mean distance is 9.54 meters, resulting in an ANN index equal to 0.061. Given
 271 that this index is less than one and almost equal to zero the CFS exhibit a clustered pattern on this micro
 272 scale of analysis. In Table 1 the ANN indices for the different priority codes and the separate zones are
 273 included as well, all resulting in a clustered pattern on point level. The more urgent calls are less
 274 clustered than priority codes 3 and 4 and of the six zones, zone West experiences the most clustered
 275 pattern.

276

277

278

Table 1

Average nearest neighbour indices

Data set	ANN	z-score
Full data set	0.061	-1344.39*
prio 0	0.39	-54.28*
prio 1	0.36	-108.94*
prio 2	0.13	-656.64*
prio 3	0.092	-940.10*
prio 4	0.16	-509.06*
North	0.057	-486.25*
East	0.078	-513.74*
South	0.082	-518.15*
West	0.032	-574.15*
City	0.055	-593.78*
Centre	0.057	-601.6*

279

* $p < 0.001$

280
 281
 282
 283
 284
 285
 286
 287
 288
 289
 290
 291
 292
 293
 294
 295
 296
 297
 298
 299
 300
 301
 302
 303

Given the absence of a peak in the z-scores for the incremental spatial autocorrelation, this tool has not led to an unambiguous result for the threshold distance. The ever-increasing z-scores could be a result of aggregating the point data to street segments, generating a too coarse aggregation level. The only lower level of analysis are the addresses, but as discussed in 2.2.1, police patrol along street segments, and some degree of aggregation is necessary to perform the Global and Local Moran’s I statistics. Hence, we will stick to this level of analysis. What we do know from this statistic is that within a threshold distance of 577 meters every feature has at least one neighbouring feature. The Global Moran’s I statistic is the highest for this threshold distance and the value slightly decreases (but still positive) as the distance increases. As shown in Table 2, the Global Moran’s I Index for this threshold distance is equal to 0.104, indicating positive spatial autocorrelation. The global Moran’s I indices for the priority codes and the six zones exhibit, in line with the ANN indices, positive spatial autocorrelation with only small variations between the indices. As with the ANN indices, prio 0 exhibits a slightly less clustered pattern than prio 3, indicating that prio 3 incidents are more clustered on both, street segment and incident level. On the level of the zones, the incidents per street segment are least clustered in North and the most in City. North is scattered over the northern part of Antwerp, which may have affected this outcome.

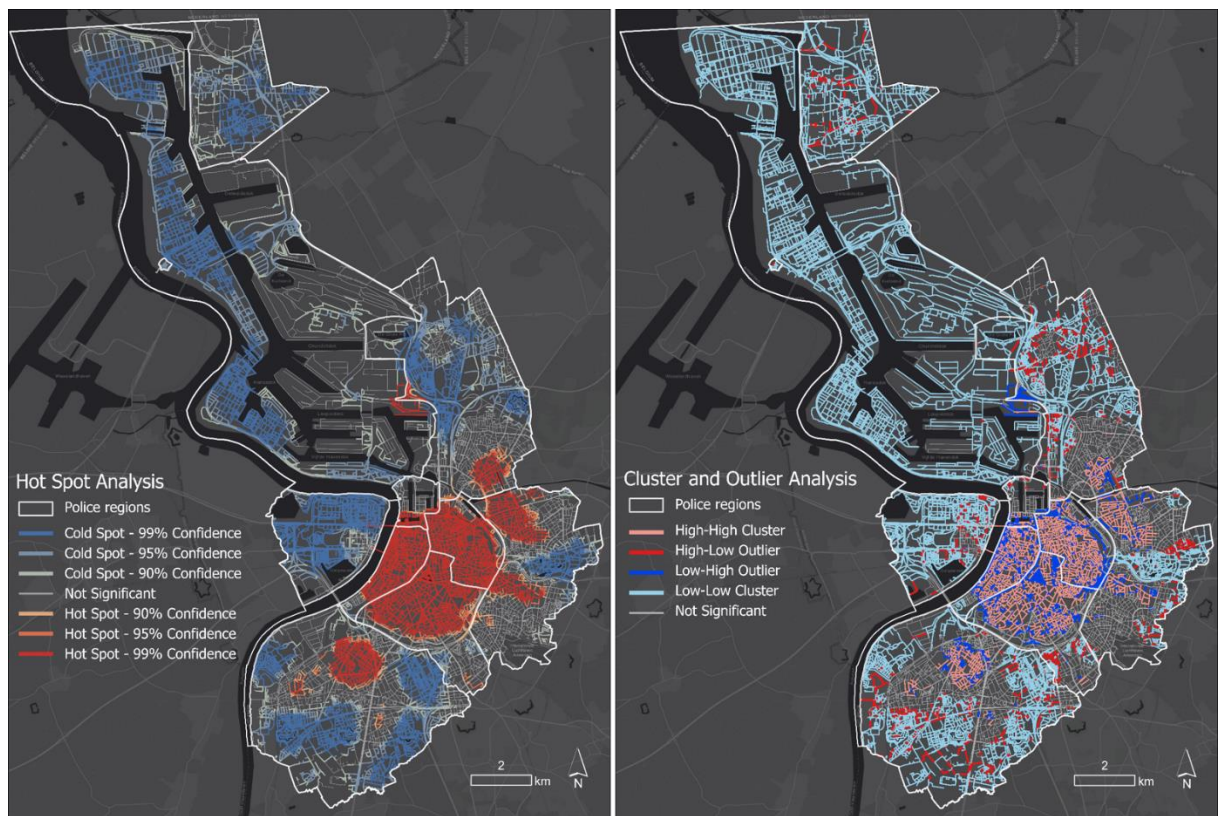
Table 2
 Global Moran’s I indices

Data set	Global Moran's I	z-score
Full data set	0.104	105.2*
prio 0	0.027	29.34*
prio 1	0.050	54.4*
prio 2	0.074	74.92*
prio 3	0.13	135.42*
prio 4	0.043	49.86*
North	0.024	15.95*
East	0.12	22.06*
South	0.075	22.73*
West	0.14	42.25*
City	0.15	18.73*
Centre	0.066	11.22*

*p < 0.001

The Gi* statistic or hot spot analysis (see, left map Fig. 3) results in four significant hot spots of CFS: the entire city centre and three clusters of street segments northeast, east, and southwest of this area. In accordance with Local Moran’s I (see, Fig. 3 right) several cold spots are scattered around the ‘hot’ city

304 centre. When we zoom in on these hot and cold spots, we can see, on the one hand, that the CFS tend to
 305 cluster (i.e., hot spots) around regional roads which connect the city centre with the surrounding districts
 306 and municipalities, around squares, in shopping streets, around the central train station, and in streets
 307 with night-time economy. On the other hand, the cold spots mainly correspond to the Zoo of Antwerp,
 308 parks, nature reserves, and the port area. The Local Moran's I statistic provides us with even more detail
 309 by showing significant outliers. Within the high-high clusters, for example, some street segments
 310 experience significantly less incidents, resulting in low-high outliers. An example of such an outlier is
 311 the dark blue triangle in the middle of the city centre. This is a park. Inversely, low-low clusters are
 312 scattered around the centrally located city centre, and are interrupted in several places by street segments
 313 with a noticeably higher frequency of incidents.
 314
 315



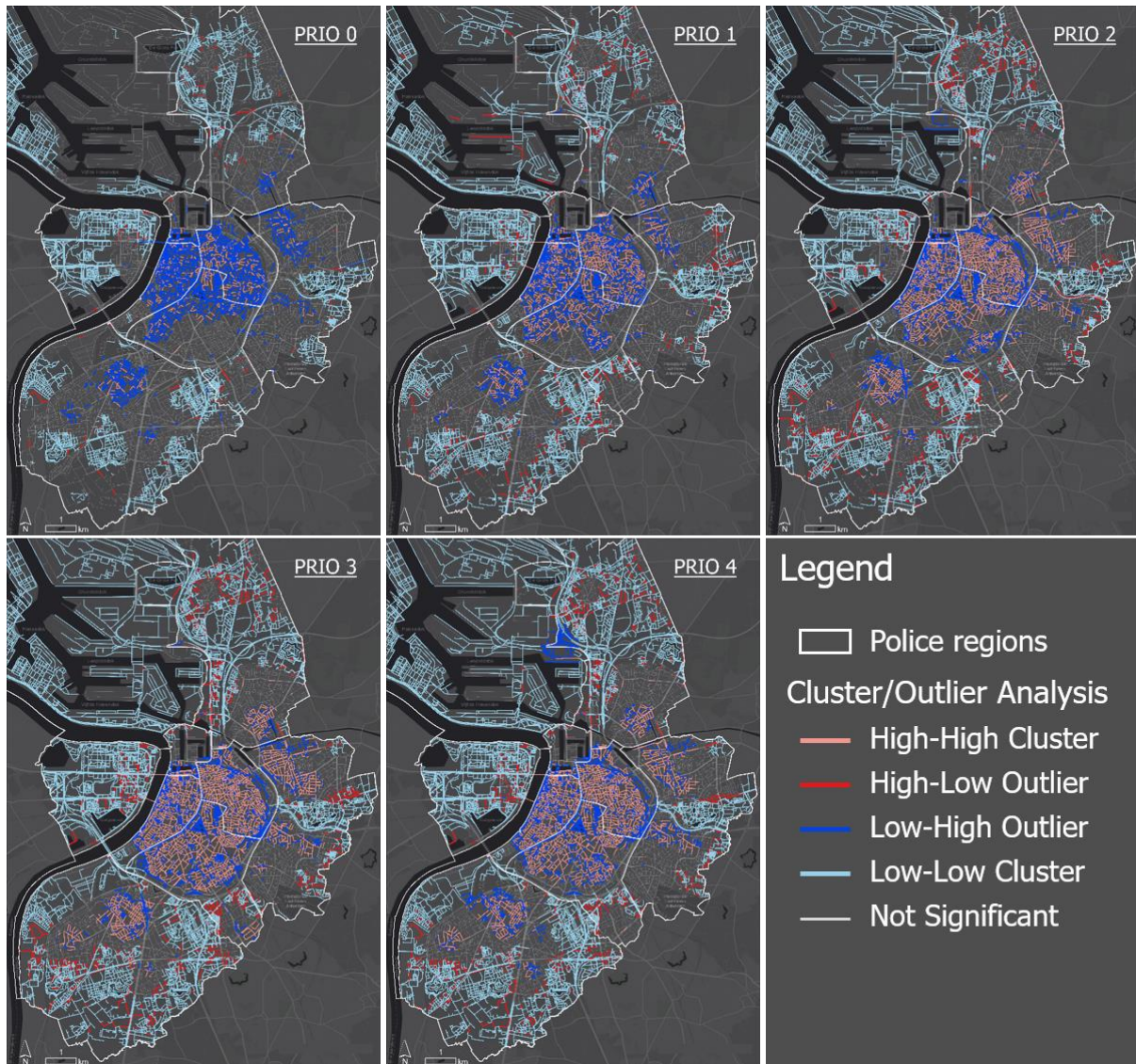
316
 317 **Fig. 3.** Getis-Ord G_i^* (left) and Local Moran's I statistic (right) of the CFS data of Antwerp, aggregated on street
 318 segment level (2017-2020).

319
 320 Fig. 4 enriches our knowledge on the level of the five priority codes. In comparison with the outcomes
 321 of Global Moran's I in Table 2, the priority codes with the highest indices, prio 2 and 3, but also 4, show
 322 a similar pattern as for all CFS (Fig. 3). In the case of priority codes 0 and 1 this pattern is less apparent.
 323 For prio 0 incidents, low-high outliers are predominant in the city centre compared to high-high clusters
 324 and the size of the clusters is notably smaller than for prio 3 or 4 CFS. In general, however, the places

325 where hot street segments or high-low outliers occur are similar for all priority codes, with a big cluster
326 in the city centre and three smaller surrounding clusters, but the higher the prio codes, the bigger the
327 size of these hot spots. The low-low clusters expand as well as the prio code increases, but they are more
328 regularly interrupted by hot street segments.

329

330



331

332 **Fig. 4.** Outcome of the Local Moran's I statistic for the CFS data per priority code (2017-2020).

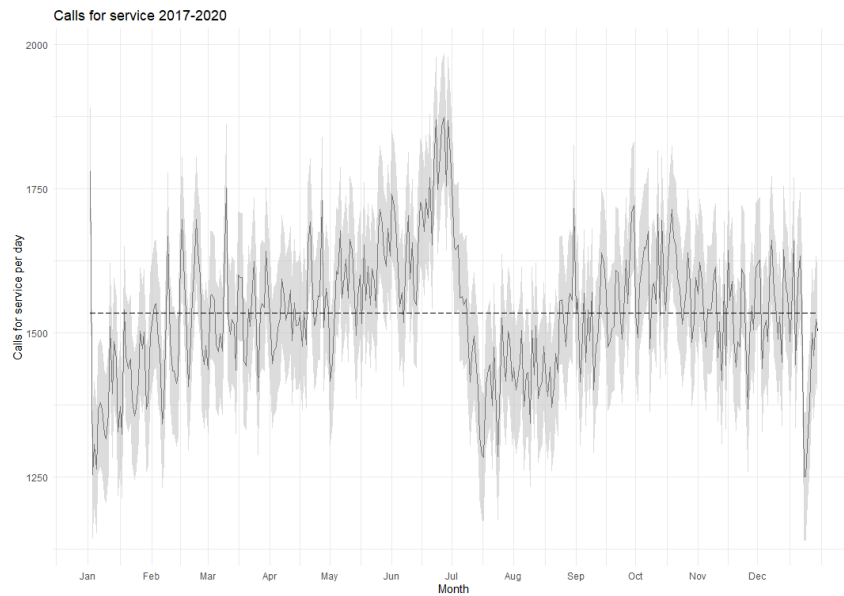
333

334 3.2 Time pattern of the emergency incident call data

335

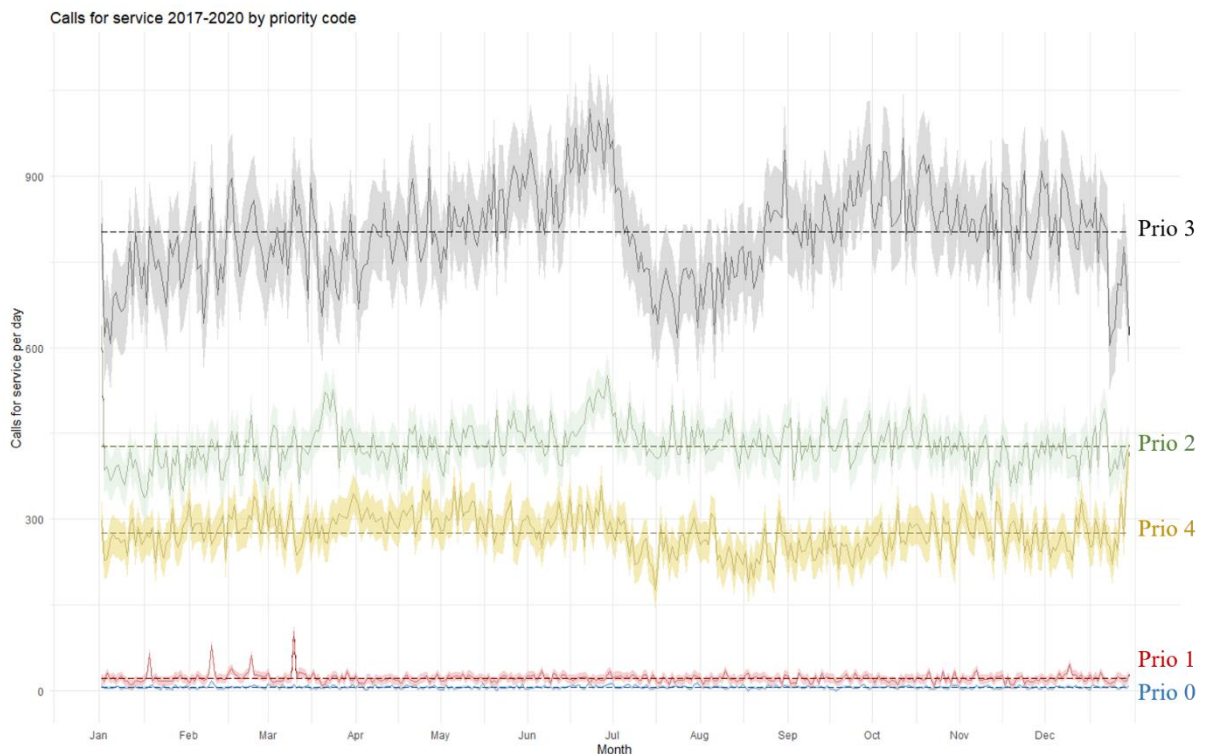
336 First, we examine the time aspect on a monthly scale of analysis. On this meso level, the pattern in Fig.
337 5 is not stable but shows an increasing pattern from the beginning of January until the end of June, which
338 is followed by a sharp decline during the summer holiday in July and August, after which the number
339 of CFS per day increases again in September, to end with a rather constant number of CFS in October,

340 November and December (cf. seasonal driver of demand). The difference in the number of CFS between
341 the different priority codes is very high, with only a small amount of urgent incidents compared to prio
342 2, 3, or 4 incidents. The curve of the prio 0 incidents shows a fairly constant pattern with no outliers. By
343 contrast, the prio 1 curve has four peaks that are the result of stormy weather with very high wind speeds.
344 Each of the four peaks can be related to storm damage caused by a storm in one of the four years in our
345 data set.
346



347
348
349

Fig. 5. Emergency call incidents per day (2017-2020).

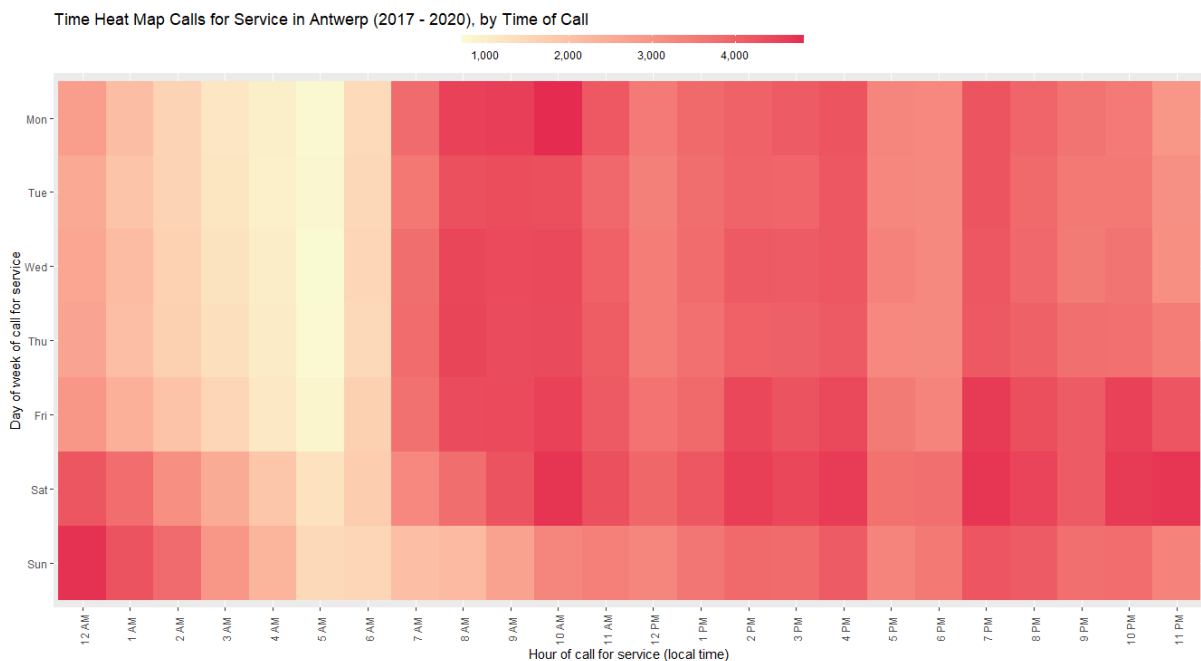


350

351
352
353
354
355
356
357
358
359
360
361
362

Fig. 6. CFS in Antwerp per day for each priority code (2017-2020).

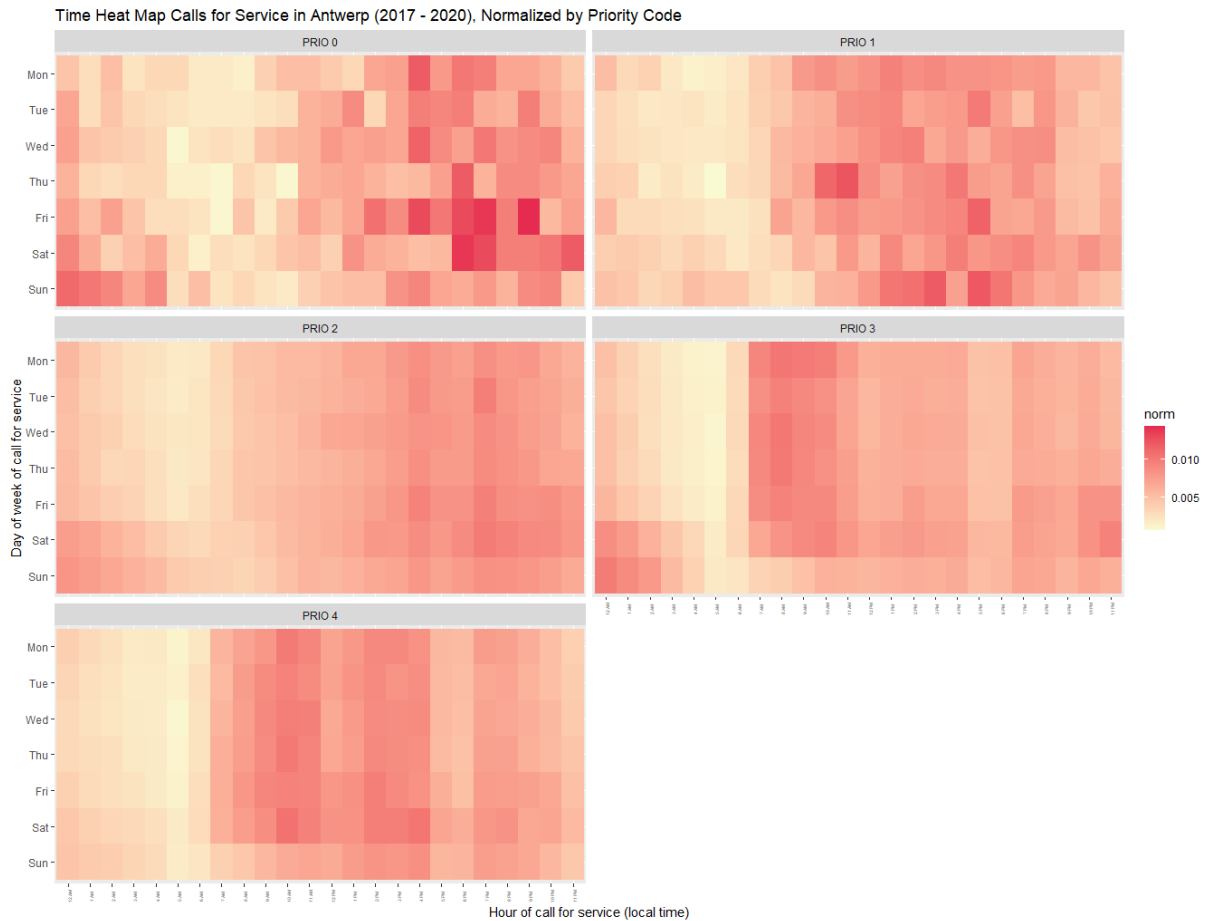
Second, Figs. 7 and 8 zoom to a smaller scale of analysis and focus on CFS by day of week and hour of day. The time heat map in Fig. 7 is generated from the CFS of the full data set. Fig. 7 gives an indication of the time pattern and allows to identify hour blocks with an increased number of incidents per hour, but does not allow to make statistically significant statements. On weekdays, CFS are elevated during morning rush hour (7 am until 12 am). On weekends and Sundays in particular, this pattern is less pronounced. Instead, Friday and Saturday evenings and nights appear to be ‘hotter’ than weeknights. Apart from the increased number of CFS during the morning rush hour, Fig. 7 also indicates a rise in incidents in the afternoon and from 7 PM until 8 PM. Across all weekdays, 5 and 6 AM is the quietest period.



363
364
365
366
367
368
369
370
371

Fig. 7. Time heat map of the CFS in Antwerp by day of week and time of day, 2017-2020.

For priority codes 0 and 1 no clear pattern can be established, however, the proportion of prio 0 calls increases on Friday evening and Saturday evening/night. The proportion of prio 2 calls rises throughout the day, with a higher proportion from 4 PM until 5 PM and from 7 PM until 8 PM, and a slightly increased proportion on Friday and Saturday evening/night. Priority codes 3 and 4 exhibit more or less the same pattern as prio 2, except for their higher proportion of CFS between 7 and 11 AM.



372

373 **Fig. 8.** Time heat map of the CFS in Antwerp by day of week and time of day per priority code, 2017-2020.

374

375 Third, the parameters of Felson and Poulsen (2003) are summarized in Table 3. The time of the first
 376 quartile minute steadily increases throughout the week; on Monday a quarter of the CFS occurs between
 377 5:00 AM and 10:50 AM, while this shifts on Sunday to 12:20 AM. The time span exhibits a similar
 378 pattern, which means that the dispersion of CFS over the day increases over the days of the week,
 379 however, on Sunday the time span is clearly shorter than on the other days. On Friday and Saturday, the
 380 time span is the longest and the 5-to-5 share of incidents the lowest. A more dispersed pattern over the
 381 day means a more clustered pattern at night, and a lower proportion of CFS between 5:00 AM and 4:59
 382 PM corresponds to a later incident pattern on Friday and Saturday, which corresponds to the increasing
 383 number of CFS on Friday and Saturday night/evening, as shown in the time heat map (Fig. 7). Moreover,
 384 these simple indicators, as they are called by Felson and Poulsen (2003), reveal differences between the
 385 temporal patterns of the priority codes. The most urgent incidents have a remarkably low 5-to-5 share
 386 of incidents and thus a clustering of CFS in the evening and night, characterised by a short time span.
 387 By 2:23 PM, only a quarter of the CFS had occurred, while on an average day this is already at 11:21
 388 AM. The time pattern of CFS with prio 1 and 2 is similar but is, especially for incidents with prio 1,
 389 slightly earlier. In contrast, prio 3 incidents have an early time pattern with a very long time span, which

390 means the CFS are spread throughout the day and evening. The highest 5-to-5 share is for prio 4 CFS;
 391 about 60% of the prio 4 CFS occur before 5 o'clock in the evening.
 392

393 **Table 3**

394 Time analysis based on the first, median, and third quartile minute, the time span, and the 5-to-5 share of crime.

day of week	First quartile minute	median minute	third quartile minute	time span (minutes)	5-to-5 share of incidents
Monday	10:50 AM	3:42 PM	8:44 PM	594	57.01%
Tuesday	10:59 AM	3:58 PM	8:59 PM	600	55.7%
Wednesday	10:57 AM	3:52 PM	8:56 PM	599	56.13%
Thursday	11:04 AM	4:07 PM	9:20 PM	616	54.59%
Friday	11:35 AM	4:59 PM	10:28 PM	653	50.07%
Saturday	11:59 AM	5:22 PM	10:52 PM	653	48.35%
Sunday	12:17 PM	4:55 PM	9:31 PM	554	50.39%
average day	11:21 AM	4:24 PM	9:37 PM	616	53.00%
prio 0	2:23 PM	6:35 PM	10:35 PM	492	39.63%
prio 1	12:10 PM	4:21 PM	8:38 PM	508,5	53.99%
prio 2	1:10 PM	5:51 PM	10:08 PM	538	45.15%
prio 3	10:40 AM	3:56 PM	9:46 PM	666	54.90%
prio 4	11:07 AM	3:23 PM	8:22 PM	555	59.89%

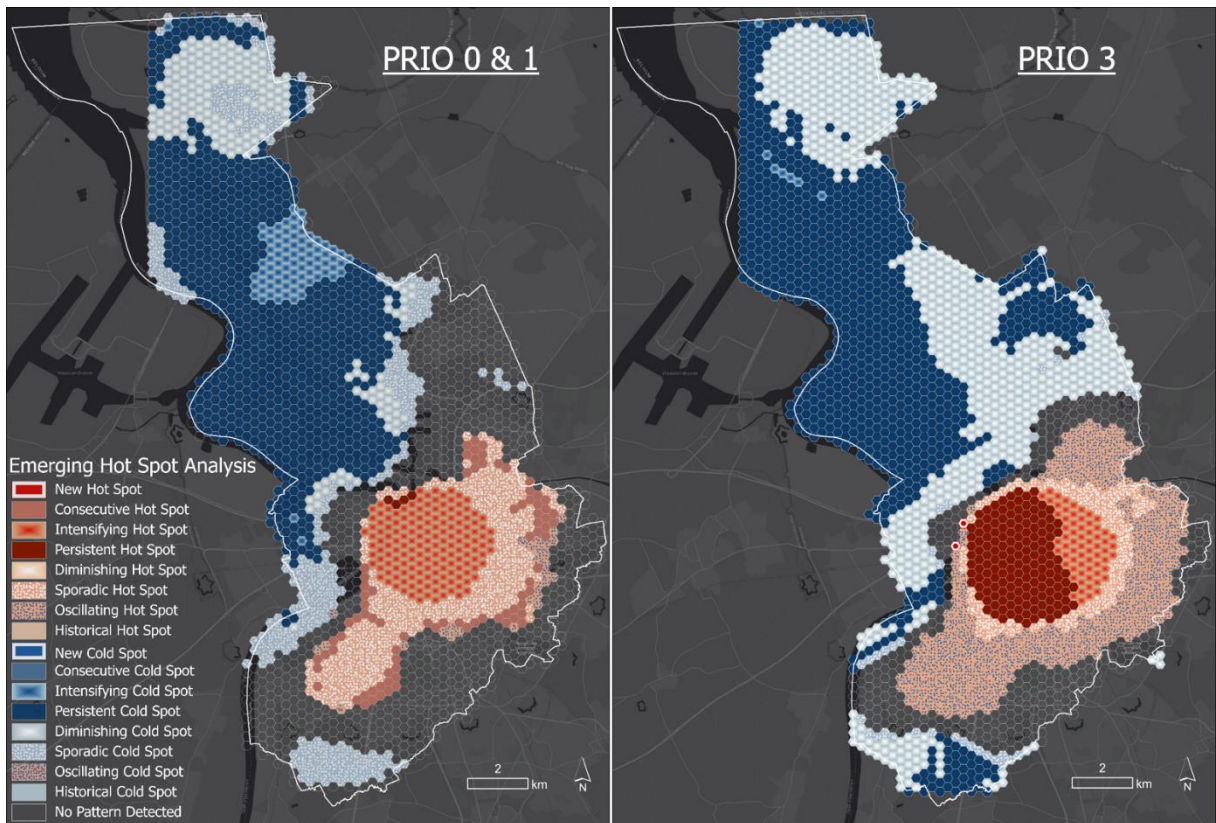
395

396 *3.3 Space-time visualisation of police demand*

397

398 Finally, the emerging hot spot analysis (see, Fig. 9) allows us to combine time and space. The bin time
 399 series in Fig. 9 consist of one day and the time-step interval is one hour. In both cases (prio 0 and 1 and
 400 prio 3), the city centre turns red, indicating the presence of significant hot spots of CFS. For the two
 401 most urgent categories, the hot spots in the city centre intensify throughout the day. This means that the
 402 hot spots in these locations are significant for ninety percent of the time-step intervals, including the
 403 final time step and the intensity of the clustering of high counts significantly increases every hour. These
 404 hot spots are surrounded by sporadic hot spots, i.e., hot spots that are alternately significant, but never a
 405 cold spot, and consecutive hot spots, i.e., locations with a single uninterrupted run of statistically
 406 significant hot spot bins in the final time-step intervals (less than ninety percent of all bins are
 407 statistically significant). Cold spots of prio 0 and 1 incidents are located in the north and south of
 408 Antwerp. The spatial pattern of hot and cold spots is similar for prio 3 incidents, although the hot spots
 409 in the city centre are mostly persistent hot spots, meaning that a location has been a statistically
 410 significant hot spot for ninety percent of the time-step intervals without a discernible trend (i.e., the
 411 number of events is high during the entire day). The hot spots surrounding these persistent hot spots are

412 mainly intensifying hot spots, sporadic hot spots, and oscillating hot spots. The oscillating hot spots
 413 were at the start of the day statistically significant cold spots, but they have turned into a statistically
 414 significant hot spot for the final hours of the day. The area occupied by this big hot spot is again much
 415 larger than for the urgent CFS. In both cases, the cold spots are predominantly persistent, except in the
 416 northernmost part of Antwerp, where the intensity of the clustering of low counts in each time step
 417 significantly decreases, but these locations are still significant cold spots.
 418



419
 420 **Fig. 9.** Emerging Hot Spots analyses of prio 0 and 1 (left) and prio 3 (right) CFS in Antwerp (2017-2020).

421
 422 The emerging hot spot maps show a more widespread occurrence of hot spots than Local Moran's I or
 423 Getis-Ord G_i^* , inter alia, because of the aggregation in hexagons. In general, we were able to detect
 424 four clusters of street segments with high levels of CFS, one big cluster representing the city centre, one
 425 in the northeast, one in the east, and one in the southwest of Antwerp.

426
 427 **4. Discussion**
 428

429 The main objective of this paper is to establish daily police demand by examining the space-time pattern
 430 of the CFS data set (2017-2020) of the Antwerp Police Department. Several exploratory (spatial) data
 431 analysis techniques are used to analyse the space, time, and space-time patterns of the overall data set
 432 and of the five priority codes. On the one hand regularities are established in the space-time pattern of
 433 the CFS. On the other hand, we detected a number of anomalies, which have to be addressed.

434

435 *4.1 A spatial perspective on calls for service*

436

437 The fact that the emergency incidents in Antwerp are clustered in time and in space is not surprising. In
438 line with other exploratory research papers on the space-time pattern of crime or CFS data, a number of
439 hot spots are detected in Antwerp. The biggest and most notable hot spot is located in the city centre of
440 Antwerp. This area contains the historical city centre, but also the main shopping streets, restaurants and
441 entertainment areas, the railway station, and lots of smaller and bigger businesses. A real central business
442 district (CBD) as there is, for example, in Barrera et al. (2013) and in Luan et al. (2016) is not clearly
443 present in Antwerp. Instead, Antwerp has over the years expanded around the old medieval city centre,
444 which is located near the river Scheldt. Barrera et al. (2013) reported clustering of several types of crimes
445 near the CBD. The concentration of offences in these areas corresponds as well to the findings of other
446 research on space-time patterns in cities. Feng et al. (2016) identified, for example, wholesale markets,
447 shopping centres, aggregation zones of passenger flows, and zones with high population mobility as
448 places with a higher number of incidents. Nakaya and Yano (2010) focused in particular on snatch-and-
449 run offences and reported clustering in the city centre and around railway stations and Luan et al. (2016)
450 also point to areas with highways, a local university, and a regional shopping centre. In the classification
451 of the drivers of police demand (see Introduction) this corresponds to the baseline (Laufs et al., 2020).

452

453 *4.2 Space-time representation of priority codes*

454

455 The prioritization of CFS and the analysis thereof is vital to organize police patrol cost-effective and
456 ethical (Kärrholm et al., 2020). Our analysis revealed that the spatial, temporal, and space-time patterns
457 of the five priority codes differ. First, the most urgent CFS, prio 0, are spatially the least clustered. The
458 hot spots are smaller and more often interrupted by street segments with a significantly lower number
459 of CFS (low-high outliers). Although the number of street segments where at least one CFS occurs is
460 much lower for prio 0 than for, e.g., prio 3 CFS (4.62% versus 35.16%, respectively), the average
461 number of incidents per segment increases much more sharply (1.5 CFS/segment versus 26.7
462 CFS/segment, respectively). Hence, the small number of prio 0 CFS is a possible explanation for the
463 limited clustering. A substantive explanation could be that these severe prio 0 CFS are rare and less
464 place and opportunity-related than the less urgent CFS. Second, the highest proportion of prio 0 incidents
465 occurred on Friday evening and Saturday evening/night and they have a later time pattern than the other
466 priority codes, which is also evidenced by the fact that the hot spots in the city centre of Antwerp become
467 more intense during the course of the day. If we compare this to prio 3 calls, we see that these clusters
468 of incidents are much bigger and a clearer time pattern can be discerned, with a higher proportion of
469 incidents on weekdays during the morning rush hour and in the weekend, on Friday and Saturday
470 evenings and nights. This also corresponds to Newton (2015) and Herrmann (2015). The former focused

471 on crime in the night-time economy, the latter, among other things, on violent crimes (murder, shootings,
472 and assaults). Both reported a significant increase in disorder starting on Friday and Saturday afternoon
473 until the early morning. Third, the drop in the number of prio 3 CFS in the summer months of July and
474 August seems to contradict research on crime seasonality, which often reports a rise in crime in the
475 summer (McDowall et al., 2011), but this may be due to a reduced morning rush hour caused by the
476 summer holiday (e.g., summer shutdown of the building sector, school holiday...). Thus, this is probably
477 caused by the type of incidents classified under prio 3, i.e., about 50% are traffic-related CFS.
478 Furthermore, prio 1 calls show a similar spatial and temporal pattern as prio 0 CFS, but the incidents
479 occur earlier in the day. The patterns of prio 2 and prio 4 calls are comparable to those of the prio 3
480 calls.

481

482 *4.3 Priority codes as an alternative to crime harm*

483

484 How crime or incident types can be valued based on their severity is studied in the crime harm literature.
485 Sherman (2013) developed the Crime Harm Index (CHI) to analyse how much harm different types of
486 crime cause by days of imprisonment. According to Weinborn et al. (2017) harm is even three times
487 more concentrated than crime counts and, therefore, the CHI is a useful statistic for crime analysis and
488 decision-making (Curtis-Ham & Walton, 2017; Kärholm et al., 2020). In the meantime, some countries
489 have already developed their own, local version of the CHI (Andersen & Mueller-Johnson, 2018; Curtis-
490 Ham & Walton, 2017; Kärholm et al., 2020); this is not yet the case for Belgium. The crime harm
491 literature states that allocating scarce police resources to harm spots instead of hot spots of crime counts
492 can prevent the more serious crimes (Kärholm et al., 2020; Sherman, 2013; Sherman et al., 2016;
493 Weinborn et al., 2017). A downside of the CHI is that it can give a distorted understanding of the
494 situation. Weinborn et al. (2017) illustrate this with an example of two places with exactly the same
495 harm values, where in one place a lot of minor incidents occurred and in another place there is one
496 incident that carries a very high penalty (e.g. homicide). If police would only focus on crime harm but
497 not on crime count, scarce resources might be allocated to tragic, yet isolated incidents. The
498 classification by priority/urgency gives, albeit in a more operational way, a similar idea of the severity
499 of CFS and also makes it possible to analyse incident count. In Antwerp, all types of CFS cluster in the
500 city centre. This is a place where a lot of people congregate and interact, resulting in crime opportunities
501 and, consequently, an increase in CFS (Fenimore, 2019; Newton, 2015). However, Fenimore (2019)
502 reported that in Washington DC more serious crimes occurred further away from the city centre.
503 Although the hot spots in our analysis are substantially smaller for the urgent incidents, the places where
504 the hot spots occur are similar. The question "where to deploy police officers" can therefore be answered
505 in the same way for all priority codes. But in Antwerp, prio 0 (and 1) CFS are given priority over the
506 other incidents and on average more vehicles are dispatched to these CFS than to CFS with a higher

507 priority code (2-3-4). In our sample, on average four police units⁹ responded to a prio 0 CFS, three to
508 prio 1, 1.5 to prio 2, and one unit to prio 3 or prio 4 calls. In 89% of the prio 0 CFS more than one unit
509 responded to the incident. This proportion slightly drops to 76% for prio 1 CFS and declines remarkably
510 for prio 2 (29%), prio 3 (9%), and prio 4 (11%) CFS. Therefore, when a prio 0 or prio 1 call occurs, it
511 will require more resources than prio 2, 3 or 4 CFS and since these CFS occur in general at a later time
512 of day and tend to cluster on Friday and Saturday night/evening, we would recommend the police to
513 respond more flexible to these increases in urgent police demand.

514

515 *4.4 Implementing prioritization in police patrol routing strategies*

516

517 A lot of police patrol routing strategies use historical crime or incident data to define patrol routes (Azimi
518 & Bashiri, 2016; Calvo et al., 2017; Chen et al., 2017). However, priority codes have never been
519 included in such a patrol strategy. Yassen et al. (2017) do define a stopping time based on the priority
520 of each hot spot, but the main objective of their routing strategy is to maximise the coverage of hot spots.
521 In other words, they do not take into account the priority of the CFS themselves and the impact on the
522 available resources. Quite often only the most urgent CFS are considered in a patrol strategy (e.g., Saint-
523 Guillain et al., 2021), which does not allow for a correct estimation of the daily demand for police (i.e.,
524 underestimation of the actual demand for police). As we demonstrate in this paper, the urgency of a CFS
525 has repercussions on the spatial and temporal distribution as well as on the operation of the police. The
526 more urgent CFS have a greater impact on patrol operation than a prio 3 or a prio 4 call. An example to
527 illustrate this: if a police zone has a call rate of six calls per hour and we know that in our case the
528 average number of responding cars per call differs depending on the priority code, the adjusted call rate
529 can be much higher than six. If six incidents with prio 3 occur, only *six* units are likely to respond, but
530 if there are 1 prio 0, 2 prio 2, 1 prio 3, and 2 prio 4 calls for service, in the worst case, *ten* units are
531 assigned (Green, 1984). Nevertheless, we cannot ignore the large differences in absolute values between
532 the priority codes. There appears to be a disparity between the incidental demand for police and the
533 structural demand for police (see, Table 4). There are 35,064 hours in our data set. Even if we weigh
534 urgent calls by the average number of vehicles responding, the number of critical CFS per hour remains
535 notably lower than for non-urgent calls. Although critical incidents are on average more demanding
536 when they occur (i.e., incidental police demand), low urgency calls take up structurally more police
537 resources (i.e., structural police demand).

538

539

540

541

542

⁹ In Antwerp, there are always two police officers per vehicle.

543
544

Table 4
CFS per hour weighted by the average number of vehicles responding

Priority codes	# CFS	# vehicles	# CFS per hour	# CFS per hour weighted by # vehicles
Prio 0	2,160	4	0.062	0.25
Prio 1	7,953	3	0.23	0.68
Prio 2	156,628	1.5	4.47	6.70
Prio 3	292,683	1	8.35	8.35
Prio 4	101,118	1	2.88	2.88

545

546 The analysis of space-time properties of priority codes and its implementation in crime prevention and
547 police patrol routing strategies have the ability, on the one hand, to prevent system overload (e.g., later
548 in the day) and, on the other hand, to avoid oversupply of police presence. We can clarify this with an
549 example of our own study area: Dau et al. (2021a) demonstrated that in Antwerp there is an overall
550 decline in the level of police deployed over the course of the day (e.g., due to staffing plans or
551 administrative work). This contradicts with our findings and indicates a possible mismatch of police
552 demand and police presence in our study area. The discovery of this misalignment highlights the added
553 value of our research for the Antwerp Police Department. Based on this example and, more in general,
554 on the findings of this paper, we would recommend to include priority codes in future police patrol
555 routing solutions to make patrol strategies more realistic. An important aspect will be to
556 increase/decrease the number of available units depending on the number of CFS per priority code.
557 Instead of only working with fixed shifts (e.g. APD), there is a need to deploy peak shifts depending on
558 the historical CFS data. This is an avenue for future research.

559

560 *4.5 Extending the framework*

561

562 To this point we have not yet questioned how we analysed ‘police demand’. In a scoping review on
563 police demand management, Laufs et al. (2020) criticize the sole focus on CFS data to study police
564 demand. They split ‘police demand’ into reactive, protective, and organisational demand. The first type,
565 reactive or public demand, is what was analysed in this paper and relates to the deployment of both
566 personnel and equipment, mostly based on CFS. However, as a result of this reactive analysis, hot spots
567 and burning times are established to then implement in preventative or proactive police work. Before
568 proactive policing can be analysed it must first be implemented in the policing strategy. Therefore,
569 spatiotemporal analysis is essential to provide police agencies with the necessary information on where
570 and when incidents occur. In a next step, the effectiveness and efficiency of the proactive patrol strategy
571 can be established. The last type of demand, organisational demand, is inherent to the organisation of
572 the police and is created by processes, protocols, administrative tasks, and bureaucracy (Laufs et al.,

573 2020). We do not have data on this type of demand, since this is beyond the scope of the current, applied
574 research objective.

575

576 *4.6 Limitations*

577

578 The objective was to fathom the space-time pattern of the entire CFS data set with a focus on the priority
579 codes, resulting in a better understanding of the overall demand for police resource. This should in turn
580 result in effective and efficient supply strategies. When comparing the findings for Antwerp – a mid-
581 sized European city – with some other study areas worldwide, similarities are evident. What stands out
582 in the other research papers on the space-time pattern of CFS is the specific focus on one or several
583 types of CFS. Although we were specifically interested in the overall, daily pattern of the calls, this can
584 be seen as a limitation of this research paper because detailed comparisons with other research papers
585 were difficult. A second limitation of our research is related to the geocoding process. We detected some
586 flaws in the geocoding algorithm that have to be solved for future analysis. These problems are caused
587 by missing information, e.g. house numbers, an exclusive focus on distance instead of on the correct
588 street name, and inaccuracies in the street segment layer. Andresen et al. (2020) discuss the fact that
589 geocoding algorithms have the potential to introduce error into analysis, but this does not by definition
590 mean that the data set is not accurate. If the flaws are random and if the geocoding match rate is above
591 85 percent, which is the case (94,79%), they conclude that the geocoded pattern is still representing the
592 actual spatial pattern (Andresen et al., 2020). Third, based on our data set the exact time when a vehicle
593 was dispatched to a CFS is known, but the underlying action could have happened before. Therefore,
594 analysing the time aspect of CFS is associated with temporal inaccuracy.

595

596 **5. Conclusions**

597

598 Information on small spatial and temporal scales of analysis, as studied here, is necessary to efficiently
599 deploy the available resources of any police force in the world. The results of this paper demonstrate
600 that even differences between the days of the week can have an impact on the daily organisation of
601 police strategies and staffing requirements. The first objective of this paper was to determine the space-
602 time pattern of the Antwerp CFS in order to improve the current patrol strategy of the Antwerp Police
603 Department to a more evidence-based and data-driven policing strategy. Antwerp is characterized by its
604 dense historical city centre, which is surrounded by the twentieth century belt where parks, residential
605 areas, and some more industrial zones alternate. This pattern is in some way reflected in the spatial
606 pattern of the demand for police: the hot city centre is surrounded by an alternating pattern of hot and
607 cold spots. The time pattern fluctuates over the months and differs on weekdays and in the weekend,
608 with clear clusters between the morning rush hour and on Friday and Saturday evening/night. Comparing
609 the space-time patterns of cities all over the world and of different sizes will improve our understanding

610 of where and when CFS cluster in time and space. In this paper similarities are detected in the space-
611 time pattern of police demand in Antwerp and in Beijing (China), Kyoto City (Japan), The Regional
612 Municipality of Waterloo (Canada), thirteen middle-sized American cities, and a study area in England.
613 Last, the analysis of the priority codes is closely related to the crime harm literature and can be used to
614 enrich research into crime harm. Our analysis of the priority codes gives insight in both, the severity of
615 an incident and the number of incidents in space and time. In turn, this information can be used in police
616 patrol routing strategies and for the efficient allocation of scarce police resources.

617

618 **References**

619

- 620 Andersen, H. A., & Mueller-Johnson, K. (2018). The Danish Crime Harm Index: How it works and
621 why it matters. *Cambridge Journal of Evidence-Based Policing*, 2(1-2), 52–69.
622 <https://doi.org/10.1007/s41887-018-0021-7>
- 623 Andresen, M. A. (2017). Mapping Crime Prevention: What We Do and Where We Need to Go. In S.
624 LeClerc (Ed.), *Crime Prevention in the 21st* (pp. 113–126). [https://doi.org/10.1007/978-3-319-](https://doi.org/10.1007/978-3-319-27793-6_9)
625 [27793-6_9](https://doi.org/10.1007/978-3-319-27793-6_9)
- 626 Andresen, M. A., & Malleson, N. (2013). Crime seasonality and its variations across space. *Applied*
627 *Geography*, 43, 25–35. <https://doi.org/10.1016/j.apgeog.2013.06.007>
- 628 Andresen, M. A., Malleson, N., Steenbeek, W., Townsley, M., & Vandeviver, C. (2020). Minimum
629 geocoding match rates: an international study of the impact of data and areal unit sizes.
630 *International Journal of Geographical Information Science*, 34(7), 1306–1322.
631 <https://doi.org/10.1080/13658816.2020.1725015>
- 632 Anselin, L. (1995). Local Indicators of Spatial Association—LISA. *Geographical Analysis*, 27(2), 93–
633 115.
- 634 Anselin, L., Cohen, J., Cook, D., Gorr, W., & Tital, G. (2000). Spatial analyses of crime. In D. Duffee
635 (Ed.), *Measurement and Analysis of Crime and Justice* (pp. 213–262). US Department of
636 Justice.
- 637 Antrop, M., Maeyer, P. de, Neutens, T., & van de Weghe, N. (2013). Metrisch-ruimtelijke analyse. In
638 M. Antrop, P. de Maeyer, T. Neutens, & N. van de Weghe (Eds.), *Geografische*
639 *Informatiesystemen* (pp. 229–284).
- 640 Ashby, M. P. J., & Bowers, K. (2013). A comparison of methods for temporal analysis of aoristic
641 crime. *Crime Science*, 2(1), 1–16.
- 642 Azimi, S. A. Z., & Bashiri, M. (2016). Modeling police patrol routing and its problem-solving
643 technique based on the ant colony optimization algorithm (case Study: Iran’s Police).
644 *Research Journal of Applied Sciences*, 11(7), 536–546.
- 645 Barrera, D. J., Cagang, S., & Capistrano, D. (2013). Spatial and temporal maps of reported crimes in
646 Dumaguete City, Negros Oriental, Philippines. *PRISM*, 18(1), 11–24.
- 647 Boivin, R. (2018). Routine activity, population(s) and crime_ Spatial heterogeneity and conflicting
648 Propositions about the neighborhood crime-population link. *Applied Geography*, 95, 79–87.
- 649 Bowers, K. (1999). Exploring links between crime and disadvantage in north-west England: an
650 analysis using geographical. *International Journal of Geographical Information Science*,
651 13(2), 159–184.
- 652 Calvo, H., Godoy-Calderón, S., Moreno-Armendáriz, M. A., & Martínez-Hernández, V. M. (2017).
653 Forecasting, clustering and patrolling criminal activities. *Intelligent Data Analysis*, 21(3),
654 697–720. <https://doi.org/10.3233/IDA-170883>
- 655 Chen, H., Cheng, T., & Wise, S. (2017). Developing an online cooperative police patrol routing
656 strategy. *Computers, Environment and Urban Systems*, 62, 19–29.
657 <https://doi.org/10.1016/j.compenvurbsys.2016.10.013>
- 658 Chun, Y. (2014). Analyzing Space–Time Crime Incidents Using Eigenvector Spatial Filtering: An
659 Application to Vehicle Burglary. *Geographical Analysis*, 46, 165–184.

- 660 Chung, J., & Kim, H. (2019). Crime Risk Maps: A Multivariate Spatial Analysis of Crime Data.
661 *Geographical Analysis*, 51, 475–499.
- 662 Curtis-Ham, S., & Walton, D. (2017). Mapping crime harm and priority locations in New Zealand: A
663 comparison of spatial analysis methods. *Applied Geography*, 86, 245–254.
664 <https://doi.org/10.1016/j.apgeog.2017.06.008>
- 665 Dau, P. M., Vandeviver, C., Dewinter, M., Witlox, F., & Vander Beken, T. (2021a). How concentrated
666 are police on crime? A spatiotemporal analysis of the concentration of police presence and
667 crime. Advance online publication. <https://doi.org/10.31235/osf.io/rxa8h>
- 668 Dau, P. M., Vandeviver, C., Dewinter, M., Witlox, F., & Vander Beken, T. (2021b). Policing
669 directions: A systematic review on the effectiveness of quantitative police presence. *European*
670 *Journal on Criminal Policy and Research*, 35. <https://doi.org/10.31235/osf.io/ezk5f>
- 671 Davies, T., & Bowers, K. (2019). Patterns in the supply and demand of urban policing at the street
672 segment level. *Policing and Society*, 30(7), 795–817.
673 <https://doi.org/10.1080/10439463.2019.1598997>
- 674 de Melo, S. N., Matias, L. F., & Andresen, M. A. (2015). Crime concentrations and similarities in
675 spatial crime patterns in a Brazilian context. *Applied Geography*, 62, 314–324.
- 676 Dewinter, M., Vandeviver, C., Vander Beken, T., & Witlox, F. (2020). Analysing the Police Patrol
677 Routing Problem: A Review. *ISPRS International Journal of Geo-Information*, 9(3), 157.
678 <https://doi.org/10.3390/ijgi9030157>
- 679 Esri ArcGIS Pro. (n.d.). *Emerging hot spot analysis (space time pattern mining)*.
680 [https://pro.arcgis.com/en/pro-app/latest/tool-reference/space-time-pattern-](https://pro.arcgis.com/en/pro-app/latest/tool-reference/space-time-pattern-mining/emerginghotspots.htm#)
681 [mining/emerginghotspots.htm#](https://pro.arcgis.com/en/pro-app/latest/tool-reference/space-time-pattern-mining/emerginghotspots.htm#)
- 682 Felson, M., & Poulsen, E. (2003). Simple indicators of crime by time of day. *International Journal of*
683 *Forecasting*, 19(4), 595–601. [https://doi.org/10.1016/S0169-2070\(03\)00093-1](https://doi.org/10.1016/S0169-2070(03)00093-1)
- 684 Feng, J., Dong, Y., & Song, L. (2016). A spatio-temporal analysis of urban crime in Beijing: Based on
685 data for property crime. *Urban Studies*, 53(15), 3223–3245.
686 <https://doi.org/10.1177/0042098015612982>
- 687 Fenimore, D. M. (2019). Mapping harmspots: An exploration of the spatial distribution of crime harm.
688 *Applied Geography*, 109, 1–10. <https://doi.org/10.1016/j.apgeog.2019.06.002>
- 689 Fondevila, G., Vilalta-Perdomo, C., Pérez, M. C. G., & Cafferata, F. G. (2021). Crime deterrent effect
690 of police stations. *Applied Geography*, 134, 11.
- 691 Fotheringham, A. S., & Wong, D. (1991). The modifiable areal unit problem in multivariate statistical
692 analysis. *Environment and Planning a*, 23(7), 1025–1044.
- 693 Getis, A., & Ord, J. K. (1992). The Analysis of Spatial Association by Use of Distance Statistics.
694 *Geographical Analysis*, 24(3), 189–206.
- 695 Goodchild, M. F. (1986). *Spatial autocorrelation*. *CATMOG: Vol. 47*. Geo Books.
- 696 Green, L. (1984). A multiple dispatch queueing model of police patrol operations. *Management*
697 *Science*, 30(6), 653–664. <https://doi.org/10.1287/mnsc.30.6.653>
- 698 Helbich, M., & Leitner, M. (2017). Frontiers in Spatial and Spatiotemporal Crime Analytics—An
699 Editorial. *ISPRS International Journal of Geo-Information*, 6(3), 73.
700 <https://doi.org/10.3390/ijgi6030073>
- 701 Herrmann, C. R. (2013). Street-Level Spatiotemporal Crime Analysis: Examples from Bronx County,
702 NY (2006–2010). In M. Leitner (Ed.), *Crime Modeling and Mapping Using Geospatial*
703 *Technologies* (pp. 73–104). Springer Netherlands. [https://doi.org/10.1007/978-94-007-4997-](https://doi.org/10.1007/978-94-007-4997-9_4)
704 [9_4](https://doi.org/10.1007/978-94-007-4997-9_4)
- 705 Herrmann, C. R. (2015). The dynamics of robbery and violence hot spots. *Crime Science*, 4(33), 1–14.
706 <https://doi.org/10.1186/s40163-015-0042-5>
- 707 Hu, Y., Wang, F., Guin, C., & Zhu, H. (2018). A spatio-temporal kernel density estimation framework
708 for predictive crime hotspot mapping and evaluation. *Applied Geography*, 99, 89–97.
709 <https://doi.org/10.1016/j.apgeog.2018.08.001>
- 710 Kärrholm, F., Neyroud, P., & Smaaland, J. (2020). Designing the Swedish Crime Harm Index: an
711 Evidence-Based Strategy. *Cambridge Journal of Evidence-Based Policing*, 4(1-2), 15–33.
712 <https://doi.org/10.1007/s41887-020-00041-4>
- 713 Kuo, P.-F., Lord, D., & Walden, T. D. (2013). Using geographical information systems to organize
714 police patrol routes effectively by grouping hotspots of crash and crime data. *Journal of*
715 *Transport Geography*, 30, 138–148.

- 716 Laufs, J., Bowers, K., Birks, D., & Johnson, S. D. (2020). Understanding the concept of 'demand' in
717 policing: a scoping review and resulting implications for demand management. *Policing and*
718 *Society*, 1–24. <https://doi.org/10.1080/10439463.2020.1791862>
- 719 Lee, Y., Eck, J. E., O, S., & Martinez, N. N. (2017). How concentrated is crime at places? A
720 systematic review from 1970 to 2015. *Crime Science*, 6(1), 1–16.
721 <https://doi.org/10.1186/s40163-017-0069-x>
- 722 Luan, H., Quick, M., & Law, J. (2016). Analyzing Local Spatio-Temporal Patterns of Police Calls-for-
723 Service Using Bayesian Integrated Nested Laplace Approximation. *ISPRS International*
724 *Journal of Geo-Information*, 5(9), 162. <https://doi.org/10.3390/ijgi5090162>
- 725 Mastrofski, S. D. (1990). Prospects of change in police patrol: A decade in review. *American Journal*
726 *of Police*, 9(3), 1–79.
- 727 McDowall, D., Loftin, C., & Pate, M. (2011). Seasonal cycles in crime, and their variability. *Journal*
728 *of Quantitative Criminology*, 28(3), 389–410. <https://doi.org/10.1007/s10940-011-9145-7>
- 729 Megler, V., Banis, D., & Chang, H. (2014). Spatial analysis of graffiti in San Francisco. *Applied*
730 *Geography*, 54, 63–73. <https://doi.org/10.1016/j.apgeog.2014.06.031>
- 731 Mukhopadhyay, A., Zhang, C., Vorobeychik, Y., Tambe, M., Pence, K., & Speer, P. (2016). Optimal
732 Allocation of Police Patrol Resources Using a Continuous-Time Crime Model. In Zhu, Q.,
733 Alpcan, T., Panaousis, E., Tambe, M., Casey, W. (Ed.), *Decision and Game Theory for*
734 *Security* (Vol. 9996, pp. 139–158). <https://doi.org/10.1007/978-3-319-47413-7>
- 735 Nakaya, T., & Yano, K. (2010). Visualising Crime Clusters in a Space-time Cube: An Exploratory
736 Data-analysis Approach Using Space-time Kernel Density Estimation and Scan Statistics.
737 *Transactions in GIS*, 14(3), 223–239. <https://doi.org/10.1111/j.1467-9671.2010.01194.x>
- 738 Nelson, A., Bromley, R., & Thomas, C. (2001). Identifying micro-spatial and temporal patterns of
739 violent crime and disorder in the British city centre. *Applied Geography*, 21(3), 249–274.
740 [https://doi.org/10.1016/S0143-6228\(01\)00008-X](https://doi.org/10.1016/S0143-6228(01)00008-X)
- 741 Newton, A. (2015). Crime and the NTE: multi-classification crime (MCC) hot spots in time and space.
742 *Crime Science*, 4(1). <https://doi.org/10.1186/s40163-015-0040-7>
- 743 Newton, A., & Felson, M. (2015). Editorial: crime patterns in time and space: the dynamics of crime
744 opportunities in urban areas. *Crime Science*, 4(1). <https://doi.org/10.1186/s40163-015-0025-6>
- 745 Ord, J. K., & Getis, A. (1995). Local Spatial Autocorrelation Statistics: Distributional Issues and an
746 Application. *Geographical Analysis*, 27(4), 286–306.
- 747 Saint-Guillain, M., Paquay, C., & Limbourg, S. (2021). Time-dependent stochastic vehicle routing
748 problem with random requests: Application to online police patrol management in Brussels.
749 *European Journal of Operational Research*, 292(3), 869–885.
750 <https://doi.org/10.1016/j.ejor.2020.11.007>
- 751 Sherman, L. W. (1995). Hot spots of crime and criminal careers of places. *Crime and Place*, 4, 35–52.
- 752 Sherman, L. W. (2013). The rise of evidence-based policing: Targeting, testing, and tracking. *Crime*
753 *and Justice*, 42, 377–343.
- 754 Sherman, L. W., Gartin, P. R., & Buerger, M. E. (1989). Hot spots of predatory crime: Routine
755 activities and the criminology of place. *Criminology*, 27(1), 27–55.
- 756 Sherman, L. W., Neyroud, P. W., & Neyroud, E. (2016). The Cambridge Crime Harm Index:
757 Measuring total harm from crime based on sentencing Guidelines. *Policing*, 10(3), 171–183.
758 <https://doi.org/10.1093/police/paw003>
- 759 Shiode, S., Shiode, N., Block, R., & Block, C. R. (2015). Space-time characteristics of micro-scale
760 crime occurrences: an application of a network-based space-time search window technique for
761 crime incidents in Chicago. *International Journal of Geographical Information Science*,
762 29(5), 697–719.
- 763 Spicer, V., Song, J., Brantingham, P., Park, A., & Andresen, M. A. (2016). Street profile analysis: A
764 new method for mapping crime on major roadways. *Applied Geography*, 69, 65–74.
765 <https://doi.org/10.1016/j.apgeog.2016.02.008>
- 766 Townsley, M. (2008). Visualising space time patterns in crime: the hotspot plot. *Crime Patterns and*
767 *Analysis*, 1(1), 61–74.
- 768 Valente, R. (2019). Spatial and temporal patterns of violent crime in a Brazilian state capital: A
769 quantitative analysis focusing on micro places and small units of time. *Applied Geography*,
770 103, 90–97. <https://doi.org/10.1016/j.apgeog.2019.01.006>

- 771 Vandeviver, C., & Bernasco, W. (2017). The geography of crime and crime control. *Applied*
772 *Geography*, 86, 220–225. <https://doi.org/10.1016/j.apgeog.2017.08.012>
- 773 Vandeviver, C., & Steenbeek, W. (2019). The (In)Stability of Residential Burglary Patterns on Street
774 Segments: The Case of Antwerp, Belgium 2005–2016. *Journal of Quantitative Criminology*,
775 35(1), 111–133. <https://doi.org/10.1007/s10940-017-9371-8>
- 776 Wain, N., & Ariel, B [B.] (2014). Tracking of Police Patrol. *Policing*, 8(3), 274–283.
777 <https://doi.org/10.1093/polic/pau017>
- 778 Watanabe, T., & Takamiya, M. (2014). Police patrol routing on network voronoi diagram.
779 *Proceedings of the 8th International Conference on Ubiquitous Information Management and*
780 *Communication*, 101, 1–8.
- 781 Weinborn, C., Ariel, B [Barak], Sherman, L. W., & O' Dwyer, E. (2017). Hotspots vs. harmspots:
782 Shifting the focus from counts to harm in the criminology of place. *Applied Geography*, 86,
783 226–244. <https://doi.org/10.1016/j.apgeog.2017.06.009>
- 784 Weisburd, D., Wyckoff, L. A., Ready, J., Eck, J. E., Hinkle, J. C., & Gajewski, F. (2006). Does crime
785 just move around the corner? A controlled study of spatial displacement and diffusion of
786 crime control benefits. *Criminology*, 44(3), 549–592.
- 787 Yassen, E. T., Arram, A., Ayob, M., & Nazri, M. Z. A. (2017). A constructive heuristic for police
788 patrol routing problems. *Science & Technology*, 25(S), 87–96.
- 789 Ye, X., Xu, X., Lee, J., Zhu, X., & Wu, L. (2015). Space–time interaction of residential burglaries in
790 Wuhan, China. *Applied Geography*, 60, 210–216.
791 <https://doi.org/10.1016/j.apgeog.2014.11.022>

792
793

794 **Declarations**

795 **Author Contributions:** Maite Dewinter: Conceptualization, Data Curation, Formal Analysis,
796 Investigation, Methodology, Visualization, Writing – original draft. Christophe Vandeviver:
797 Conceptualization, Validation, Supervision, Writing – review & editing, Funding Acquisition.
798 Philipp M. Dau: Writing – review & editing. Tom Vander Beken: Supervision, Funding
799 Acquisition. Frank Witlox: Supervision, Writing – review & editing, Funding Acquisition.

800

801 **Funding:** This work was supported in part by the Ghent University Research Council (UGent-
802 BOF) Interdisciplinary Research Project funding scheme [BOF18/IOP/001 to C.V., T.V.B.,
803 F.W.]. Christophe Vandeviver's contribution was supported by the Research Foundation—
804 Flanders (FWO) Postdoctoral Fellowship funding scheme [12CO619N to C.V.]. FrankWitlox's
805 contribution was supported by the Estonian Research Council [PUT PRG306 to F.W.].

806

807 **Acknowledgments:** We would like to thank the Antwerp Police Department (APD) for
808 providing us with the anonymized data set.

809

810 **Conflicts of Interest:** The authors declare no conflict of interest.

811

812 **Disclaimer:** Points of view and interpretations of data and results expressed in this research
813 paper represent a consensus of the named authors and do not necessarily represent the official

814 position or policies of the Antwerp Police Department (APD). Although a thorough quality
815 check was executed, the APD give no warranty in regard to the correctness and completeness
816 of the provided datasets.
817